Bremsstrahlung Yield of High-Energy Electrons in Hydrogen*

DAVID BERNSTEIN AND W. K. H. PANOFSKY
High-Energy Physics Laboratory and Department of Physics, Stanford University, Stanford, California
(Received January 12, 1956)

The bremsstrahlung yield of 500- and 550-Mev electrons for the production of 235-Mev photons has been measured in liquid hydrogen. The photons are traced via the production of positive photopions in liquid hydrogen. The result demonstrates a cross section $(2.4\pm2.8)\%$ below the calculations of Wheeler and Lamb. The result can be accounted for by (a) the exchange effect between the final electrons, and (b) interference effects among the protons and electrons in molecular hydrogen. A calculation on the latter effect has been carried out using Heitler-London wave functions.

A. INTRODUCTION

THE production of electromagnetic radiation due to high-energy electrons in hydrogen is characterized by the large contribution of electron-electron collisions to the yield. The measurement of the radiative cross section in hydrogen is thus concerned with different questions than is the measurement in heavier elements.[1,2] For heavier elements, the point in question is the validity of the Born approximation; for hydrogen the interest lies in the yield from *e-e* collisions.

The relative yield of radiation from the proton and the electron depends in detail on the screening calculations, which in turn are dependent on the incident and final electron energies. The method chosen here fixes the photon energy by using positive-pion production at a fixed angle and energy as a "tracer" on the photon energy.

A calculation in Born approximation of the theoretical bremsstrahlung cross section of electrons in hydrogen has been made by Wheeler and Lamb[3] (hereafter called "W.-L."). The W.-L. calculation makes the following approximations: (a) Momentum transfers to the electron larger than mc are neglected. (b) Exchange effects—i.e., effects due to the identity of the two final electrons—are neglected. (c) Atomic (not molecular) hydrogen wave functions are used in the calculation of the atomic form factors.

The first approximation has been shown to be valid if accuracies of 1% are considered. Calculations on the exchange effect have been carried out by Votruba[4] for the case of e^+-e^- pair production by photons in the field of an unscreened electron. Rohrlich and Joseph[5] have extended Votruba's calculation to hydrogen by correcting the W.-L. calculations in terms of the final recoil electron distribution of Votruba.[4] The exchange effect turns out to be fairly large: it reduces the cross section by roughly 10%.

B. EXPERIMENTAL METHOD

The external beam of the energy-analyzed electron beam of the Stanford Mark III linear accelerator[6] is passed through a long, liquid-hydrogen target (15-in. length of hydrogen). Positive pions of 68-Mev kinetic energy produced in a short length of this target are counted using an experimental arrangement previously described.[7,8] The target is mounted on accurately machined "ways" which permit translating the target by a known amount. If the translation is such that the short length from which pions are observed remains within the hydrogen, then the excess yield observed when the target is moved toward the source of electrons is caused by the photons produced in the extra length of hydrogen corresponding to the translation. This additional pion yield can then be compared with the count produced by photopions from the radiation of a copper radiator.

The method of translating a hydrogen target was chosen in preference to introducing a separate hydrogen radiator since the translation method makes the result independent of the amount of radiating material in the beam and independent of the geometrical boundaries of the liquid hydrogen.

Figure 1 indicates schematically the three conditions in which pion counts were taken. In position H, the hydrogen target acts as both radiator and target. In position Cu, a known copper radiator is introduced. In position O, pions are produced due to (1) residual radiation of the electron beam in windows, air, remaining hydrogen, etc., and (2) the direct production of pions by electrons.[8]

If C_H, C_{Cu}, and C_O are the counting rates under the conditions indicated, then the number $N_k^{(H)}$ of photons produced in a distance d of liquid hydrogen (where d is

* The research reported here was supported by the joint program of the Office of Naval Research and the U. S. Atomic Energy Commission.
[1] P. C. Fisher, Phys. Rev. **92**, 420 (1953).
[2] K. L. Brown (to be published).
[3] J. A. Wheeler and W. E. Lamb, Phys. Rev. **55**, 858 (1939). Professor Wheeler has kindly notified us of a small correction in the scale of the "inelastic" curve of Fig. 1 of this paper, we have used the corrected curves.
[4] V. Votruba, Bull. Intern. Acad. Tschèque sci. **49**, 19 (1948); results outlined in Phys. Rev. **73**, 1468 (1948).
[5] F. Rohrlich and J. Joseph, Phys. Rev. **100**, 1241(A) (1955).
[6] M. Chodorow *et al.*, Rev. Sci. Instr. **26**, 134 (1955).
[7] Crowe, Friedman, and Motz, Phys. Rev. **98**, 268(A) (1955); and to be published.
[8] Panofsky, Newton, and Yodh, Phys. Rev. **98**, 751 (1955); Panofsky, Woodward, and Yodh (to be published).

the target translation) is related to the number $N_k^{(Cu)}$ of photons produced by the copper radiator, and the number $N_k^{(air)}$ of photons produced in a distance d of air by the relation

$$Y=\frac{N_k^{(H)}-N_k^{(air)}}{N_k^{(Cu)}}=\frac{C_H-C_O}{C_{Cu}-C_O}. \quad (1)$$

The experiment was designed so that Y is near unity; under these conditions no corrections for thick-target effects are necessary; the only geometrical parameters which have to be measured with some precision are the value of the displacement d and the surface density of the copper radiator.

C. EXPERIMENTAL ARRANGEMENT

Figure 2 shows the detailed experimental arrangement. The beam was monitored by two independent

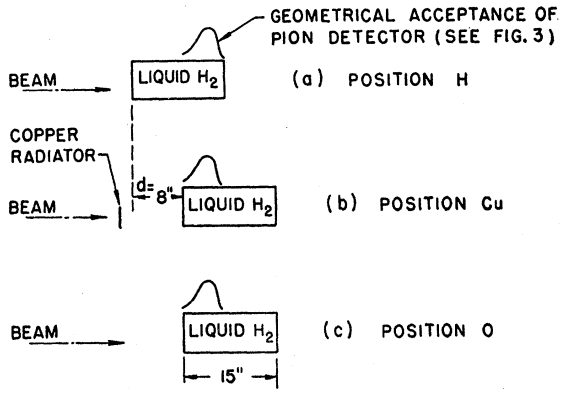

FIG. 1. Illustration of the three configurations of radiator, liquid-hydrogen target, and geometrical acceptance of the meson detector. Positions are as follows: (a) position H: target "upstream"; hydrogen makes large contribution to radiation; (b) position Cu: target "downstream"; copper radiator in place; (c) position O: target "downstream"; no additional radiator. Acceptance profile (see Fig. 3) and target displacement are to scale along the beam axis. The acceptance profile is plotted on a logarithmic amplitude scale (similar to Fig. 3).

secondary-electron monitors described elsewhere.[9] The pion-detecting apparatus, consisting of a momentum-analyzing channel and plastic-scintillator detector, has also been described previously.[7,8] The electronics was modified somewhat from the previous arrangement: counts were recorded simultaneously in four delayed-time gates after the beam pulse and in three integral-discriminator channels.

The liquid-hydrogen target has an inner cup of styrofoam of 15-in. length, 3-in. width, and $6\frac{3}{4}$ in. height. The electron beam passes $1\frac{1}{2}$ in. above the bottom of the cup. The cup is placed in a double-walled styrofoam container. The long side walls of the styrofoam container are jacketed with liquid nitrogen. The

[9] G. W. Tautfest and H. R. Fechter, Rev. Sci. Instr. 26, 229 (1955).

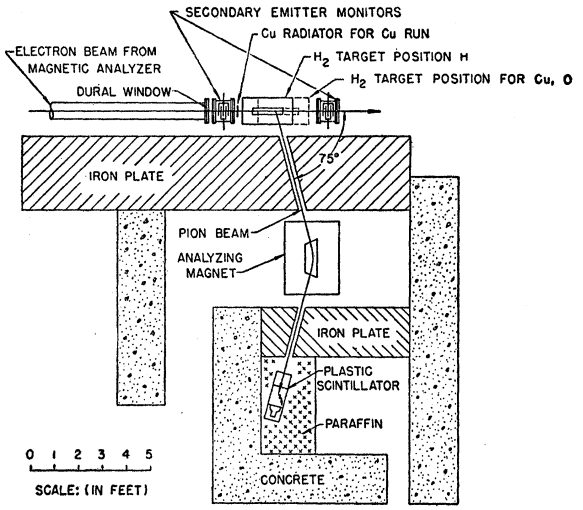

FIG. 2. Pion-detecting apparatus shown relative to target configurations.

total consumption rate of the target, including transfer losses, is 3 liters/hour, approximately. The target slides in dovetailed ways; the displacement d is measured by a gauge block.

The geometrical acceptance of the meson detecting channel was measured in separate experiments by translating a thin copper target along the beam axis. Figure 3 shows a typical profile. As a result of this profile, it was felt that a value of $d=8$ in. would give a safe margin for containing the acceptance profile fully in the 15-in. hydrogen region.

D. RESULTS

The results given here were obtained in two independent sets of runs. In the first set A, the primary electron energy was set at 550 Mev; in the second set B, at 500 Mev.

The runs were programmed so as to achieve a rotation of counts in positions H, Cu, and O in order to cancel

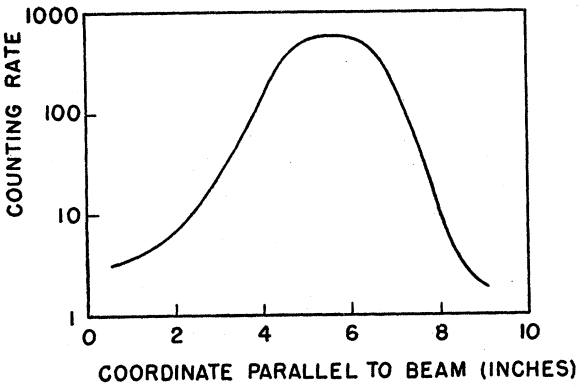

FIG. 3. Pion acceptance profile of pion-detecting equipment of Fig. 2. Counting rates are plotted on a logarithmic scale as a function of the position of a thin target displaced along the beam axis.

TABLE I. Tabulation of counts obtained for the various radiator and target configurations given in Fig. 1. The quantity Y (see text) is evaluated separately for each of the 22 counting cycles; the variation in Y is compared with the expected variation based on counting statistics.

Run	Position H Counts	Position H Monitor units	Position Cu Counts	Position Cu Monitor units	Position O Counts	Position O Monitor units	$Y\pm\epsilon$	$\frac{\lvert Y-\bar{Y}\rvert}{\epsilon}$	$\left(\frac{Y-\bar{Y}}{\epsilon}\right)^2$
	1026	200	508	100	363	100	1.033±0.195	1.275	1.62
	969	200	1024	200	331	100	0.852±0.115	0.591	0.35
	1012	200	1080	200	336	100	0.834±0.103	0.484	0.23
A	966	200	1082	200	336	100	0.718±0.097	0.682	0.46
	1000	200	1070	200	302	100	0.850±0.080	0.800	0.64
	1036	200	1164	200	353	100	0.721±0.091	0.693	0.49
	1975	400	2193	400	331	100	0.769±0.070	0.214	0.04
	1902	400	4014	750	296	100	0.874±0.052	1.730	3.00
							$\bar{Y}_A=0.782\pm0.031$		$\sum_1^n\left(\frac{Y-\bar{Y}}{\epsilon}\right)^2=6.83$
									$(n-1)^{-1}\sum_1^n\left(\frac{Y-\bar{Y}}{\epsilon}\right)^2=0.98$
	423	200	486	200	95	100	0.792±0.097	0.464	0.21
	466	200	530	200	150	100	0.722±0.116	0.216	0.05
	440	200	527	200	219	150	0.621±0.133	0.948	0.90
	483	200	521	200	169	101	0.796±0.161	0.304	0.09
	392	200	966	401	383	250	0.489±0.129	2.000	4.00
	904	400	422	200	134	100	1.195±0.228	1.970	3.90
B	896	400	1004	392	347	200	0.554±0.117	1.650	2.72
	825	400	900	400	278	200	0.779±0.108	0.296	0.09
	951	400	1270	500	352	200	0.795±0.131	0.366	0.13
	1563	600	995	400	332	200	1.135±0.137	2.460	6.03
	1404	600	1131	400	364	200	0.515±0.090	2.600	6.80
	1152	500	973	400	335	200	0.877±0.135	0.963	0.93
	935	422	959	400	327	200	0.766±0.131	0.145	0.02
	252	100	1004	400	159	100	1.011±0.225	1.174	1.39
							$\bar{Y}_B=0.788\pm0.032$		$\sum_1^n\left(\frac{Y-\bar{Y}}{\epsilon}\right)^2=21.23$
									$(n-1)^{-1}\sum_1^n\left(\frac{Y-\bar{Y}}{\epsilon}\right)^2=1.63$

possible systematic errors due to drifts in counter efficiency, gate timing, etc.

Table I shows the data obtained. The results are tabulated in terms of 22 separate measurements of the ratio Y. Each value of Y is evaluated together with its individual standard deviation ϵ based on counting statistics alone. The average value of $\bar{Y}$ is computed from the measurements of series A and B. In order to test whether any fluctuations beyond those accountable by counting statistics are present, Table I also includes a column of the values of $[(Y-\bar{Y})/\epsilon]^2$, i.e., the square of the deviation from the mean in units of the statistical standard deviation. The sum of this quantity should be equal to the number of entries minus one.

Series A gives a value of $\bar{Y}_A=0.782\pm0.031$ while series B gives a value of $\bar{Y}_B=0.788\pm0.032$ based on counting statistics alone.

The theoretical variation of the ratio of the hydrogen to copper cross sections (see below) is very insensitive to either the initial or final electron energies. Hence the two runs do not contain information as to the energy variation of the process; in the discussion we will treat the combined information.

The primary energy is known to $\pm0.5\%$. The pion energy is taken as $T_\pi=68\pm5$ Mev corresponding to a photon energy of 234 ± 6 Mev. The uncertainties quoted affect the theoretical values of the ratio Y by less than 0.1%.

E. DISCUSSION

1. Comparison with W.-L. Theory

Based on the W.-L. theory, the radiative cross sections are then given in Table II. Taking these figures in relation to the Bethe-Heitler[10,11] values of the radiative cross sections in copper and air, we can compute a predicted value of Y corresponding to the radiator thickness (0.337 g/cm^2) chosen and corresponding to the value of d, taken as 8.007 in.±0.007 in. In addition, we take the copper radiative cross section 1.3% lower than the Bethe-Heitler value; this is based on the theorem of Olsen[12] connecting the total cross sections of bremsstrahlung and electron-pair production and

[10] H. A. Bethe and W. Heitler, Proc. Roy. Soc. (London) **A146**, 83 (1934).
[11] H. A. Bethe, Proc. Cambridge Phil. Soc. **30**, 524 (1934).
[12] H. Olsen, Phys. Rev. **99**, 1335 (1955).

TABLE II. Comparison of the measured value of $\bar{Y}$ [see Eq. (1)] with the W.–L. value $Y_{\text{W.–L.}}$. The W.–L. radiation cross section $\varphi_{\text{W.–L.}}$ and the radiation cross section in copper $\varphi_k^{(\text{Cu})}$ are also tabulated.

Run	E	$\bar{Y}_{\text{exp}}$	$\varphi_{\text{W.–L.}}\times10^{29}$ cm^2	$\varphi_k^{(\text{Cu})}\times10^{26}$ cm^2	$Y_{\text{W.–L.}}$	$\bar{Y}_{\text{exp}}/Y_{\text{W.–L.}}$
A	550 Mev	0.782±0.031	10.58	3.36	0.807	0.969±0.038
B	500 Mev	0.788±0.032	10.29	3.28	0.802	0.983±0.040
						Mean=0.976±0.028

the well-known deviation from Born approximation of the experimental measurements of the pair-production cross section.[13] Recent measurements by Brown[2] at this laboratory support this correction. As the result of these calculations we obtain the values of $Y_{\text{W.–L.}}$ entered in Table II. Hence the mean of the ratios of the experimental to the W.–L. values of Y is given by

$$M=0.976\pm0.028. \tag{2}$$

2. Calculation of the Effect of the Structure of the Hydrogen Molecule

Kinematically, the minimum momentum transfer in the radiation of a photon of energy k by an electron of incident energy E_0 and rest mass μ can easily be shown to be

$$q_{\min}=k\mu^2/[2E_0(E_0-k)]. \tag{3}$$

Hence, as is well known, in the high-energy relativistic limit the minimum momentum transfer is not limited by the kinematics but by the screening effect of the atomic electrons. For the parameters used here, $q_{\min}$ is roughly equal to 500 ev so that screening is essentially complete. However, an appreciable contribution to the cross section will originate from momentum transfers q such that $\hbar/q$ will be comparable to molecular dimensions. Hence, interference effects between the individual nuclei and electrons in the molecule are not necessarily negligible. This effect is of course most pronounced in hydrogen where all the available electrons are bonding electrons.

The interaction corresponding to a given momentum transfer q in the Coulomb field (taking $\hbar=c=1$) due to m nuclei of Z atomic number and n electrons at position R_i and r_i, respectively, is given by

$$J=\int e^{i\mathbf{q}\cdot\mathbf{r}}\left(\sum_{i=1}^{m}\frac{Z_ie^2}{|\mathbf{r}-\mathbf{R}_i|}-\sum_{i=1}^{n}\frac{e^2}{|\mathbf{r}-\mathbf{r}_i|}\right)d\mathbf{r}$$
$$=\frac{4\pi e^2}{q^2}\left(\sum_{i=1}^{m}Z_ie^{i\mathbf{q}\cdot\mathbf{R}_i}-\sum_{i=1}^{n}e^{i\mathbf{q}\cdot\mathbf{r}_i}\right). \tag{4}$$

The matrix element leading from an initial molecular state ψ_0 to a final state ψ_f is thus given by

$$M=\frac{4\pi e^2}{q^2}\int\psi_f^*\left(\sum_{i=1}^{m}Z_ie^{i\mathbf{q}\cdot\mathbf{R}_i}-\sum_{i=1}^{n}e^{i\mathbf{q}\cdot\mathbf{r}_i}\right)$$
$$\times\psi_0d\mathbf{r}_1\cdots d\mathbf{r}_nd\mathbf{R}_1\cdots d\mathbf{R}_m. \tag{5}$$

[13] See, e.g., DeWire, Ashkin, and Beach, Phys. Rev. **83**, 505 (1951).

The transition probability corresponding to a given momentum transfer $\mathbf{q}$ is then proportional to the square of the modulus of this matrix element summed over final states. Applying the closure theorem, we obtain for this probability:

$$P=\left(\frac{4\pi e^2}{q^2}\right)^2\int\psi_0^*\left|\sum_{i=1}^{m}Z_ie^{i\mathbf{q}\cdot\mathbf{R}_i}-\sum_{i=1}^{n}e^{i\mathbf{q}\cdot\mathbf{r}_i}\right|^2$$
$$\times\psi_0d\mathbf{r}_1\cdots d\mathbf{r}_nd\mathbf{R}_1\cdots d\mathbf{R}_m. \tag{6}$$

Note that the use of the closure theorem generates an expression (6) which includes, as well as elastic processes, processes leading to electron excitation or ejection, and processes leading to molecular excitation or dissociation.

Equation (6) can be evaluated for the case of the hydrogen molecule. Figure 4 shows the coordinates used, following the notation of Pauling and Wilson.[14] Let us use the molecular wave functions according to the Heitler-London[15] approximation. In terms of the atomic ground-state function

$$u(r)=\frac{\exp(-r/a_0)}{a_0^{\frac{3}{2}}\sqrt{\pi}}, \tag{7}$$

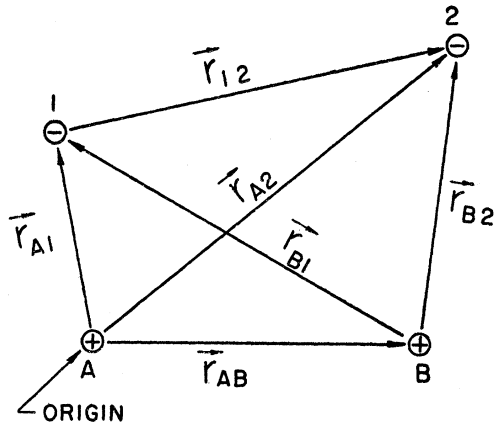

FIG. 4. Illustration of the coordinate system used in describing the hydrogen molecule. A and B are the protons and 1 and 2 the electrons. Proton A serves as origin for the position coordinates used in the text.

[14] L. Pauling and E. B. Wilson, *Introduction to Quantum Mechanics* (McGraw-Hill Book Company, Inc., New York, 1935), pp. 340 ff.

[15] W. Heitler and F. London, Z. Physik 44, 455 (1927).

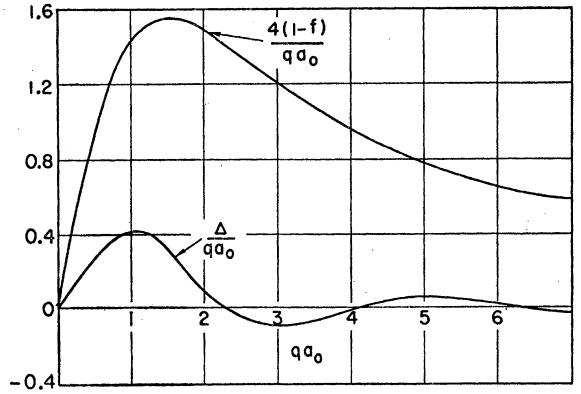

FIG. 5. Contribution of various momentum transfers q to the radiation cross section in hydrogen. The function $[4(1-f)/qa_0]dq$ represents the contribution to the cross section of two *separate* hydrogen atoms in the range q and $q+dq$ of momentum transfer to the Coulomb field. The function $(\Delta/qa_0)dq$ represents the corresponding difference in contribution between the hydrogen molecule and two separate hydrogen atoms. Momentum transfers are in units of $\hbar/a_0$ where a_0 is the Bohr radius.

where a_0 is the Bohr radius, we therefore put

$$\psi_0=\left\{\frac{[u_A(r_1)u_B(r_2)+u_B(r_1)u_A(r_2)]}{\sqrt{2}(1+I^2)^{\frac{1}{2}}}\right\}\times\delta(\mathbf{R}_1)\delta(\mathbf{R}_2-\mathbf{r}_{AB}), \quad (8)$$

where u_A and u_B are the function (7) referred to A and B as origins, respectively, and where

$$I=\int u_A(r)u_B(r)d\mathbf{r}=e^{-D}[1+D+(D^2/3)], \quad (9)$$

is the "overlap integral," and $D=r_{AB}/a_0$.

We are taking the nuclei to be at fixed coordinates, thus ignoring the effect of the spatial extent of the nuclear wave functions in the molecular ground state.

With this wave function, the transition probability P in Eq. (6) can be evaluated easily. We shall give the result as the difference Δ between P evaluated for the hydrogen molecule and P evaluated for two hydrogen atoms. We obtain

$$\Delta\equiv P(H_2)-2P(H)=\frac{2q^2-4Ig+4fI^2}{1+I^2}+\frac{2\sin(qr_{AB})}{qr_{AB}(1+I^2)}\times[(1+I^2)-2f-2Ig-f^2], \quad (10)$$

in terms of the overlap integral I given by (5), the "atomic form factor" f given by

$$f=\int u(r)e^{iq\cdot r}u(r)d\mathbf{r}=[1+(qa_0/2)^2]^{-2}, \quad (11)$$

and the "form factor overlap" g given by

$$g=\int u_A(r)u_B(r)e^{iq\cdot r}d\mathbf{r}=\left\{\frac{e^{-D}}{[1+(qa_0/2)^2]^2}\right\}\left\{1+\frac{D[1-\cos(qa_0D)]}{(q^2a_0^2D^2/2)}+\left(\frac{2}{q^2a_0^2}-\frac{1}{2}\right)\left[1-\frac{\sin(qa_0D)}{qa_0D}\right]\right\}. \quad (12)$$

Figure 5 shows the numerical values of Δ and $2P(H)$ as a function of the momentum transfer q. Equation (10) can be used to compute the bremsstrahlung cross sections for any combination of photon and electron energies by integrating the product of the momentum transfer probabilities computed here with the differential radiation cross sections as derived by Bethe and Heitler[10] and Bethe.[11]

In the particular region of parameters of interest in this experiment, screening is essentially complete ($q_{\min}\approx 0$), and hence the correction to the W.–L. formula becomes

$$\varphi(H_2)-2\varphi(H)=4\alpha Z^2r_0^2\left(\frac{dk}{E_0^2k}\right)\left[(E_0^2+E^2-\tfrac{2}{3}E_0E)\int_0^\infty\Delta(q)\frac{dq}{q}\right], \quad (13)$$

where r_0 is the classical electron radius and α is the fine-structure constant. Numerical evaluation of the integral in Eq. (13) gives

$$[\varphi(H_2)-2\varphi(H)]/2\varphi(H)=0.027. \quad (14)$$

This result is energy-independent as long as screening is complete. This effect is thus barely significant here.

3. Contribution Due to Exchange

Calculations on the effect of exchange between the two final electrons in the case of pair production in the field of a free electron have been carried out by Votruba.[4] Using his result Rohrlich and Joseph calculated the exchange effect on the total cross section for pair production in a hydrogen atom; they found[5]

$$\frac{\varphi_{\text{exchange}}-\varphi_{\text{no exchange}}}{\varphi_{\text{no exchange}}}=-0.091\pm 0.011. \quad (15)$$

As long as no calculation on the exchange effect in bremsstrahlung for the particular photo energy used is available, the above value for pair production can be used as a crude estimate.

4. Comparison between Theory and Experiment

From the previous discussion, we expect the measured value of Y to be $(6.4\pm 1.2)\%$ less than the W.–L. predicted values. Our experimental result (Table II) is

$(2.4\pm2.8)\%$ less than the W.-L. result. We therefore conclude that theory and experiment are in substantial agreement, but that the corrections discussed are significant.

We should like to point out that considerations similar to those discussed here apply also to pair-production and multiple Coulomb scattering problems.

F. ACKNOWLEDGMENTS

We are pleased to acknowledge the help given to us by K. L. Brown, A. J. Lazarus, and G. B. Yodh during the execution of the experiment. The pion-detecting equipment was substantially identical to that used in previous experiments at this laboratory, as developed principally by K. M. Crowe. S. W. Lee aided in the design of the target-translation system.

We are indebted to the operating and maintenance crews of the Mark III linear accelerator for their valuable contribution.

We are grateful to Professor F. Rohrlich for informing us of the status of the calculations on the exchange contribution to the production in hydrogen; J. J. Tiemann contributed to the numerical work in reducing Eq. (13). We are greatly indebted to Professor R. Feynman for valuable discussion on the exchange contribution.

PHYSICAL REVIEW VOLUME 102, NUMBER 2 APRIL 15, 1956

High-Energy Electron-Nuclear Scattering

H. MENDLOWITZ
National Bureau of Standards, Washington, D. C.
(Received December 1, 1955)

The Hamiltonian of a Dirac electron is transformed to a representation in which an expansion in inverse powers of the kinetic energy is facilitated. The approximation of Yennie, Ravenhall, and Wilson is readily obtained and correction terms of order $(m/p)^2$ indicated. At lower energies, it is shown that the scattering gives the gross aspects rather than the details of the charge distribution, as is well known. Effects of the spin-dependent terms in the interaction are discussed.

I. INTRODUCTION

THERE has been a great deal of interest[1,2] recently in high-energy electron scattering from nuclei in order to obtain more information regarding the charge distribution within the nucleus. Yennie *et al.*[2] have done a phase-shift calculation for an electron in the electromagnetic potential of a static spherically symmetric charge distribution. Inelastic scattering with nuclear excitation was not considered, and quantum electrodynamic radiative corrections were neglected. A detailed account was given of the scattering theory for the Dirac equation in which the mass term vanishes. This approximation is valid for electron energies high compared with the rest mass of the electron.

In this note we will discuss another representation of the Hamiltonian for a Dirac particle in an electrostatic potential field. The effects of neglecting the mass term will be indicated quite readily and the magnitudes of correction terms will be noted.

II. HAMILTONIAN

The Dirac equation for a particle in a potential field V is given in Hamiltonian form by

$$E\psi=H_D\psi=[\boldsymbol{\alpha}\cdot\mathbf{p}+\beta m+V]\psi, \quad \hbar=c=1, \qquad (1)$$

where $\boldsymbol{\alpha}$ and β are the usual Dirac four-by-four matrices. Since the α_i and β matrices cannot all be diagonal, there is a mixing of the four-component spinor ψ by the Hamiltonian in Eq. (1).

Foldy and Wouthuysen[3] have shown, by performing a canonical transformation, that for a free particle they can separate the four-component spinor into two two-component spinors. For low energies, these two-component spinors can be associated with positive- and negative-energy states. They were able to take into account interactions with electromagnetic fields by expanding the Hamiltonian in terms of the inverse rest energy. This approximation is valid for energies small compared with the rest energy. Case[4] generalized the Foldy-Wouthuysen transformation for particles with spin other than $\frac{1}{2}$. The main feature of this transformation is that a representation is found in which there is no mixing of the components of the four-component Dirac spinor (spin $\frac{1}{2}$ particle) by the field-free Hamiltonian; and when there are interacting fields, they are able to express the Hamiltonian in a manner such that the major effects of the Hamiltonian do not include the mixing of the two two-component spinors and the amount of mixing can be readily ascertained. Kurşunoğlu[5] found a unitary transforma-

[1] Lyman, Hanson, and Scott, Phys. Rev. **84**, 626 (1951); Pidd, Hammer, and Raka, Phys. Rev. **92**, 436 (1953); Hofstadter, Hahn, Knudsen, and McIntyre, Phys. Rev. **95**, 512 (1954); L. I. Schiff, Phys. Rev. **92**, 988 (1953).
[2] Yennie, Ravenhall, and Wilson, Phys. Rev. **95**, 500 (1954).
[3] L. L. Foldy and S. A. Wouthuysen, Phys. Rev. **78**, 29 (1950).
[4] K. M. Case, Phys. Rev. **95**, 1323 (1954).
[5] B. Kurşunoğlu, Office of Scientific Research Technical Note 55-336 (unpublished). (I am indebted to Dr. M. Danos for bringing this report to my attention.)